

Dynamic Simulation of Squirrel Cage Induction Machine-A Simplified and Modular Approach

Omonowo (David) Momoh

Indiana University-Purdue University Fort Wayne, Indiana, USA

Abstract

This paper presents an easy to understand dynamic simulation model of Induction Machine Model on Simulink/MATLAB software platform. A somewhat different induction machine model equations in which flux linkage equations are expressed in terms of reactances rather than inductances is used. Also, the model equations for the three phase carrier-based pulsewidth voltage source inverter for driving the induction machine are presented in a comprehensible and detailed manner. The Simulink blocks developed are divided into fifteen sub-systems with each sub-system solving one of the model equations in a detailed, easy to understand form. The results obtained correlates with the results obtained using inductance based flux linkage approach and those obtained in the original paper.

1. Introduction

In many applications, the dynamic behavior of the induction machines has an important effect upon the overall performance of the system of which it is a part [1]. Dynamic simulation of induction machines using Simulink allows the transient behavior to be studied. The use of Simulink for dynamic simulation of electrical system places it at an advantage over other circuit simulators that shows only the steady state behavior of the circuit. Simulink is an extension of MATLAB that allows engineers to rapidly and accurately build computer models of dynamical systems using block diagram notation [2]. The block diagram notation for modeling complex nonlinear systems makes Simulink an effective analytical tool for engineering technology students.

A model of the induction motor and other electric machine models are available in the Simulink Power System Blockset, these models provide access to a

limited number of machine parameters [3]. Also, many Simulink induction machine models in existence do not give detailed explanation concerning how the model equations are derived and simulated. In most cases, the authors skip many steps thereby leaving the readers to figure out the missing links. While this approach may be considered justifiable for experts in the field due to the nature of their training, it is imperative and necessary that detailed, more comprehensive and clearer model equations be presented in works that focus on engineering students that are just learning to develop research tools in electrical machine analysis.

This work is a reproduction of part of earlier work done in [4]; it is also an extension of the earlier work done by this author in [5]. The motivation for embarking on reproducing the original paper stems from the fact that similar results obtained in [4] can be achieved using a more simplified and understandable but yet shorter method. The author in [3] has also made a commendable attempt in simplifying the work done in [4], but he failed to include the model equations for the inverter drive employed for his machine. In this work, the model equations for the three phase carrier-based pulsewidth voltage source inverter are developed and presented in a clear and easily implementable manner. The approach adopted in [6] is employed to develop the model equations for the three phase voltage source inverter. Also, the induction machine model equations are restructured in such a way that makes it easier for engineering and technology students to follow.

In this paper, the Simulink model is configured into sub-systems, with each subsystem solving one model equations in a comprehensive and easy to understand form. A double – click on each of the subsystem gives a detailed model equation and the machine parameters used. The method used to transform the voltages and currents from their natural (ABC) form to the synchronously rotating reference frame (dq) form in the original paper was somehow long and strenuous. The authors first transformed the three – phase voltages to a

two – phase stationary reference frame (V_{qs}^s and V_{ds}^s), and thereafter multiply by unit vector block to achieve the desired synchronously rotating reference frame transformation. In this paper, a more straight forward method was used by choosing the reference frame transformation speed (angle) that is equal to the fundamental frequency (speed) of the variables (voltages and currents) associated with the rotating circuits [8, 9]. Also, the flux linkages are expressed in terms of reactances rather than inductances. This is achieved by simply multiplying the inductances by the base speed of the inductance machine.

2. Model Equations

2.1. Modelling of Carrier-Based Voltage-Source Inverter

The turn-on and turn-off of the switching semiconductor devices on the three phase voltage source inverter are represented by an existence function. The existence function has a value of unity and zero when the device is turned and turned off respectively [6]. The existence function can be designated as S_{ij} where $i = a, b, c$ represents each of the three phases and $j = p, n$, represents the top and bottom switches on any of the three inverter legs respectively.

In other to avoid short circuit on any of the inverter legs, Kirchhoff's Voltage Law (KVL) must be obeyed in the operation of the switching devices. Consequently the existence function must be constrained as follows:

$$S_{ip} + S_{in} = 1 \quad (1)$$

The voltage between the i^{th} inverter phase and the center point of the dc-link capacitor otherwise known as the switched inverter phase voltage is related to the inverter output phase voltage as follows:

$$v_{io} = v_{in} + v_{no} \quad (2)$$

where v_{io} is the switched inverter phase voltage, v_{in} is the inverter output voltage, and v_{no} is the neutral voltage. Also, there is a relationship between the inverter switched voltage, the existence functions, and the dc bus voltage as follows:

$$v_{io} = \frac{1}{2} v_{dc} (S_{ip} - S_{in}) \quad (3)$$

where v_{dc} is the dc bus voltage.

From (1),

$$S_{in} = 1 - S_{ip} \quad (4)$$

By substituting (4) into (3), we have the following:

$$v_{io} = \frac{1}{2} v_{dc} (2S_{ip} - 1) \quad (5)$$

For the three phase voltage source inverter, incorporating (2) with (5) translates to

$$\begin{aligned} v_{an} + v_{no} &= \frac{1}{2} v_{dc} (2S_{ap} - 1) \\ v_{bn} + v_{no} &= \frac{1}{2} v_{dc} (2S_{bp} - 1) \\ v_{cn} + v_{no} &= \frac{1}{2} v_{dc} (2S_{cp} - 1) \end{aligned} \quad (6)$$

The Fourier series approximation of the existence function are approximated as follows [6, 7]

$$S_{ip} = 0.5(1 + m_{ip}) \quad (7)$$

For the three phase inverter, this translates to

$$\begin{aligned} s_{ap} &= 0.5(1 + m_{ap}) \\ s_{bp} &= 0.5(1 + m_{bp}) \\ s_{cp} &= 0.5(1 + m_{cp}) \end{aligned} \quad (8)$$

m_{ap} , m_{bp} , and m_{cp} are the respective carrier-based modulation waveforms for each of the three phases. The magnitude ranges between 1 and -1 and are made up of fundamental frequency components [6]. These modulation signals are compared with the carrier signal such that the switches turn on when the magnitude of the corresponding modulation signal is greater than the triangle carrier signal and vice versa.

For a balanced system, the equation for the modulation signal for the top switching devices can be obtained by combining (5) and (7) as follows:

$$m_{ip} = \frac{v_{ip}}{0.5v_{dc}} \quad (9)$$

where m_{ip} is the magnitude of the phase modulation signal, v_{ip} is the magnitude of the fundamental inverter output phase voltage and v_{dc} is the dc bus voltage.

2.2. Induction Machine-Synchronous Reference Frame Transformation

The output phase voltages from the voltage source inverter are used to drive the induction motor. The three phase voltages feeding the stator of the induction motor are:

$$V_{as} = V_{ms} \cos(\omega_e t) \tag{10}$$

$$V_{bs} = V_{ms} \cos(\omega_e t - \beta) \tag{11}$$

$$V_{cs} = V_{ms} \cos(\omega_e t + \beta) \tag{12}$$

The rotor voltage equations referred to the stator side are:

$$V'_{ar} = \frac{N_s}{N_r} V_{mr} \cos(\omega_e t) \tag{13}$$

$$V'_{br} = \frac{N_s}{N_r} V_{mr} \cos(\omega_e t - \beta) \tag{14}$$

$$V'_{cr} = \frac{N_s}{N_r} V_{mr} \cos(\omega_e t + \beta) \tag{15}$$

The solution of the voltage equation is very involving and complex due to the fact that some of the machine inductances (self and mutual) are functions of the rotor speed which automatically make them time varying. This undesirable feature can be eliminated by a proper change of variables which in effect transforms the voltages and currents of both the stator and rotor to a common frame of reference [1]. Also, reference frame transformation of induction machines' voltage, current and flux linkage equations, allows for the controllability induction machine like their direct current (dc) machine counterpart. Power electronics converters have made induction machine control easy and it has relatively replaced dc machine. In vector control, the induction motor is run like a separately excited dc motor [10]. Although, the transformed equations of induction machines are now developed in the 'one size fits them all' reference name otherwise known as arbitrary reference, type of reference frame transformation would need to be specified during simulation .

The synchronous reference frame was used in this work. It has the unique property that during balanced steady steady state operation, the system variables (voltages, currents, and flux linkages) are constants [11]. The stator and rotor referred voltages in synchronous reference frame is as expressed in equation (16) and (17) respectively.

$$\begin{bmatrix} V_{qs} \\ V_{ds} \end{bmatrix} = K(\theta_e) \begin{bmatrix} V_{as} \\ V_{bs} \\ V_{cs} \end{bmatrix} \tag{16}$$

$$\begin{bmatrix} V'_{qr} \\ V'_{dr} \end{bmatrix} = K(\theta_e) \begin{bmatrix} V'_{ar} \\ V'_{br} \\ V'_{cr} \end{bmatrix} \tag{17}$$

$$K(\theta_e) = \frac{2}{3} \begin{bmatrix} \cos(\theta_e) & \cos(\theta_e - \beta) & \cos(\theta_e + \beta) \\ \sin(\theta_e) & \sin(\theta_e - \beta) & \sin(\theta_e + \beta) \\ \frac{1}{2} & \frac{1}{2} & \frac{1}{2} \end{bmatrix} \tag{18}$$

$$\theta_e = \int \omega_e dt + \theta(0) \tag{19}$$

The quadrature and direct axes equivalent circuit for the induction motor are shown in Fig. 1 and Fig. 2 respectively.

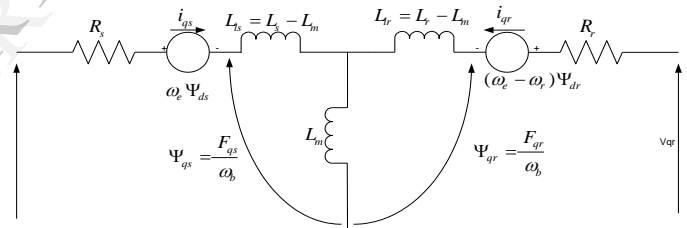


Fig.1. q – axis equivalent circuit of an induction machine

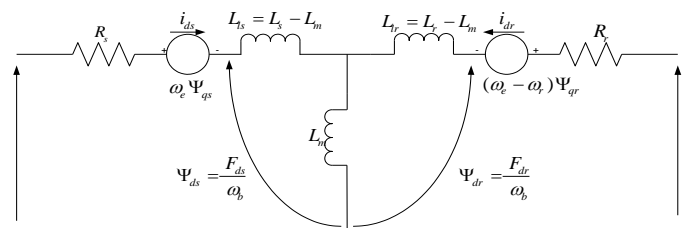


Fig.2. d – axis equivalent circuit of an induction machine

3. Voltages and Flux Linkages Equations

Based on the equivalent circuits of Fig.1 and Fig.2, the following equations for stator and rotor referred voltages and flux linkages for dynamic simulation are obtained.

$$V_{qs} = r_s I_{qs} + \frac{\omega}{\omega_b} F_{ds} + \frac{1}{\omega_b} p F_{qs} \quad (20)$$

$$V_{ds} = r_s I_{ds} - \frac{\omega_e}{\omega_b} F_{qs} + \frac{1}{\omega_b} p F_{ds} \quad (21)$$

$$V'_{qr} = r'_r I'_{qr} + \frac{(\omega_e - \omega_r)}{\omega_b} F'_{dr} + \frac{1}{\omega_b} p F'_{qr} \quad (22)$$

$$V'_{dr} = r'_r I'_{dr} - \frac{(\omega_e - \omega_r)}{\omega_b} F'_{qr} + \frac{1}{\omega_b} p F'_{dr} \quad (23)$$

$$p F_{qs} = \omega_b \left[V_{qs} - \frac{\omega_e}{\omega_b} F_{ds} + \frac{r_s}{x_{ls}} (F_{mq} - F_{qs}) \right] \quad (24)$$

$$p F_{ds} = \omega_b \left[V_{ds} + \frac{\omega_e}{\omega_b} F_{qs} + \frac{r_s}{x_{ls}} (F_{md} - F_{ds}) \right] \quad (25)$$

$$p F'_{qr} = \omega_b \left[V'_{qr} - \frac{(\omega_e - \omega_r)}{\omega_b} F'_{dr} + \frac{r_r}{x_{lr}} (F_{mq} - F'_{qr}) \right] \quad (26)$$

$$p F'_{dr} = \omega_b \left[V'_{dr} + \frac{(\omega_e - \omega_r)}{\omega_b} F'_{qr} + \frac{r_r}{x_{lr}} (F_{md} - F'_{dr}) \right] \quad (27)$$

For a squirrel cage induction machine (which is the case in this paper), V'_{qr} and V'_{dr} in equations (22), (23), (26) and (27) are set to zero since the rotor bars are short-circuited at the end ring.

The equations for self and mutual flux linkages are given as follows:

$$F_{qs} = x_{ls} I_{qs} + x_m (I_{qs} + I'_{qr}) = x_{ls} I_{qs} + F_{mq} \quad (28)$$

$$F_{ds} = x_{ls} I_{ds} + x_m (I_{ds} + I'_{dr}) = x_{ls} I_{ds} + F_{md} \quad (29)$$

$$F'_{qr} = x'_{lr} I'_{qr} + x_m (I_{qs} + I'_{qr}) = x'_{lr} I'_{qr} + F_{mq} \quad (30)$$

$$F'_{dr} = x'_{lr} I'_{dr} + x_m (I_{ds} + I'_{dr}) = x'_{lr} I'_{dr} + F_{md} \quad (31)$$

$$F_{mq} = x'_{ml} \left[\frac{F_{qs}}{x_{ls}} + \frac{F'_{qr}}{x'_{lr}} \right] \quad (32)$$

$$F_{md} = x'_{ml} \left[\frac{F_{ds}}{x_{ls}} + \frac{F'_{dr}}{x'_{lr}} \right] \quad (33)$$

$$x'_{ml} = \frac{x_m x'_{lr} x_{ls}}{(x_{ls} x'_{lr} + x_m x'_{lr} + x_m x_{ls})} = 1 / \left(\frac{1}{x_{ls}} + \frac{1}{x'_{lr}} + \frac{1}{x_m} \right) \quad (34)$$

4. Electromagnetic Torque Equations

The torque equations are given in equations (35) and (36).

$$T_e = \frac{3}{4} P \frac{1}{\omega_b} (F_{ds} I_{qs} - F_{qs} I_{ds}) \quad (35)$$

$$T_e - T_L = \frac{2J}{P} p \omega_r \quad (36)$$

5. Simulation Results

The Simulink block developed for the simulation of the induction motors is shown in Fig. 3.

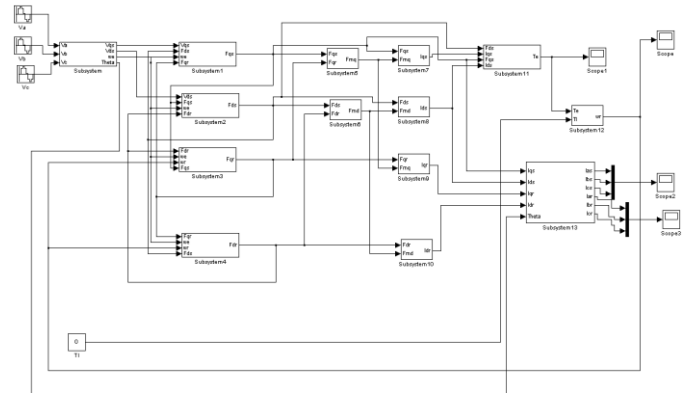


Fig.3. Simulink block for three phase voltage source inverter driven squirrel cage induction motor simulation

Equations (1) through (9) are used for the Simulink simulation of the three phase carrier-based PWM voltage source inverter. The magnitude and frequency of the modulation signals are 0.8 and 60 Hz

respectively. The dc bus voltage utilized to realize the 180 V input voltage to the motor is 450 Vdc. This can be determined using (9). The inverter output phase voltages for the three phases are shown in Fig. 4. It can be seen from figure 4 that each output phase voltage exhibits three-steps in their respective quarter-cycle. This is a characteristic of a three phase, two-level, voltage-source inverter and it confirms the switching operations in each of the three-legs of the inverter.

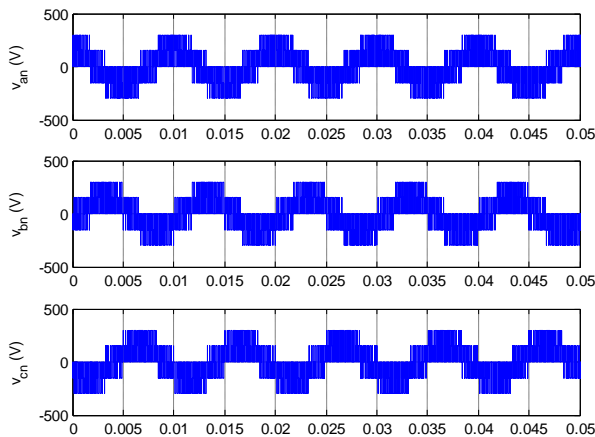


Figure 4. Inverter output phase voltages

The simulations results for direct - on – line starting of the induction motor showing plots of stator current, electromagnetic torque, and rotor speed at no load and at load are shown below.

Figure 5 shows the plot of the combined three phase stator currents of the induction motor. The figure shows a slight change in the stator current when a 50 Nm load torque was applied 0.16 second.

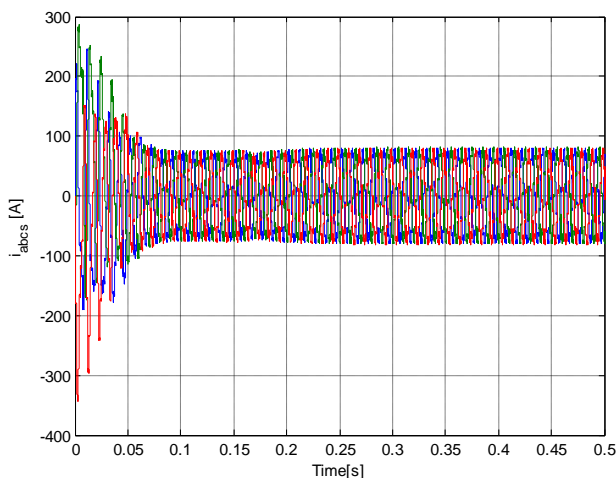


Fig.5. Plots of combined stator current versus time

Figure 6 shows the plot of the electromagnetic torque of the induction motor. It can be seen from the figure that the machine has reached steady state at about 0.14 second. A 50 Nm load torque was applied to the machine at 0.16 second. The figure shows how the electromagnetic torque rises from zero to 50 Nm to counter the 50 Nm load torque applied and a new steady state established.

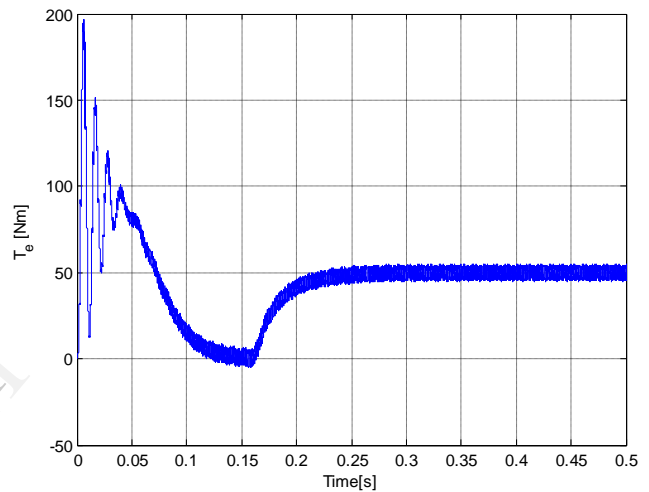


Fig.6. Plot of electromagnetic torque versus time

Figure 7 shows the rotor speed versus time. The figure shows how the rotor speed dropped from the synchronous value of 625 rad/s at no load to about 525 rad/s when the 50 Nm load was applied at 0.16 second.

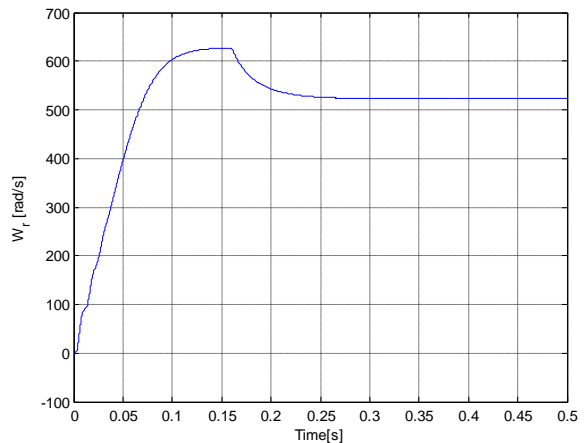


Fig.7. Plot of rotor speed versus time

Figure 8 shows the plot of the combined three phase rotor currents of the induction motor. At steady state following the free acceleration, rotor currents become zero. However, at 0.16 second when the 50 Nm load torque was applied, there is current flowing in the rotor due to the applied load. In practical situation, damper windings are incorporated in the rotor to suppress this current.

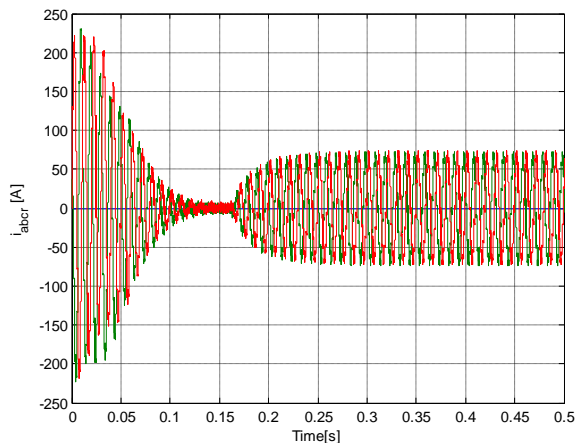


Fig.8. Plots of combined rotor current versus time

6. Conclusions

A simplified method of dynamic simulation of squirrel cage induction motor using Simulink has been implemented in this work. Modeling of the machine equations was done in a detailed and easy to understand fashion. A somewhat different induction machine model equations in which flux linkage equations are expressed in terms of reactances rather than inductances was used. The model equations for the three phase PWM voltage-source inverter was also developed. The model equations were grouped into modules. Each module was implemented using a subsystem in the Simulink block. The results obtained agree with those of earlier work done in references [3] and [4]. However, the approach presented in this work is more detailed, simpler and shorter.

7. References

- [1] P. C. Krause, and C. H. Thomas, "Simulation of symmetrical induction machinery," *IEEE Trans. Power Apparatus and Systems*, vol. PAS-84, no. 11, pp. 1038-1053, 1965.

- [2] J. B. Dabney, and T. L. Harman, "Mastering Simulink," Upper Saddle River, NJ: Pearson / Prentice Hall, 2004, pp. 1-6
- [3] A. W. Leedy, "Simulink/MATLAB dynamic induction motor model for use in undergraduate electric machines and power electronics courses," in *Proc. 2013 IEEE Southeastern Symposium on System Theory (SSST)*, pp. 1-6.
- [4] B. Ozpineci, and L. M. Tolbert, "Simulink implementation of induction machine model – a modular approach," in *2003 Proc. IEEE Int. Conf. Electric Machine and Drives (IEMDCap03)*, pp. 728-734.
- [5] O. D. Momoh, "Dynamic simulation of cage rotor induction machine – A simplified and modular approach," in *Proc. 2012 IEEE Southeastern Symposium on System Theory (SSST)*, pp. 200-203.
- [6] O. Ojo, "The generalized discontinuous PWM three-phase voltage source inverters," *IEEE Transactions on Industrial Electronics*, vol. 51, no. 6, 2004, pp. 1280-1289.
- [7] S. Karugaba, and O. Ojo, "A carrier-based modulation technique for balanced and unbalanced reference voltages in multiphase voltage-source inverters," *IEEE Transactions on Industrial Electronics*, vol. 48, no. 6, 2012, pp. 2102-2109.
- [8] P. C. Krause, O. Wasynczuk, S. D. Sudhoff, "Analysis of Electric Machinery and Drive Systems," 2nd ed. M. E. El-Hawary, Ed. Wiley – Interscience, 2002, pp. 109–187.
- [9] C-M. Ong, *Dynamic Simulation of Electric Machine using Matlab / Simulink*. Upper Saddle River, NJ: Prentice Hall, 1998, 167-180.
- [10] A. S. Nanoty, and A. R. Chudasama, "Design of multiphase induction motor for electric ship propulsion," *IEEE 2011 Electric Ship Technologies Symposium (ESTS)*, 2011, pp. 283-287.
- [11] P. C. Krause, F. Nozari, T. L. Skvarenina, and D. W. Olive, "The theory of neglecting stator transients," *IEEE Trans. Power Apparatus and Systems*, vol. PAS-98, no. 1, pp.141-148, 1979.

8. Appendix

V_{ms} = magnitude of stator voltage.

V_{mr} = magnitude of rotor voltage.

$\beta = 120^\circ$ (three – phase)

N_s = Number of turns of stator windings

N_r = Number of turns of rotor windings

$K(\theta_e)$ = synchronous reference frame transformation

matrix.

ω_e = synchronous speed (stator angular electrical frequency)

θ_e = synchronous angle.

$\theta(0)$ = phase angle

F_{mq} = q axis magnetizing flux linkages

F_{md} = d axis magnetizing flux linkages

x_{ls} = stator leakage reactance ($\omega_e L_{ls}$)

x_{lr} = rotor leakage reactance ($\omega_e L_{lr}$)

F_{qs} = q – axis stator self-magnetizing flux linkages

F_{ds} = d – axis stator self-magnetizing flux linkages

F_{qr} = q – axis rotor self-magnetizing flux linkages

F_{dr} = d – axis rotor self-magnetizing flux linkages

x_m = magnetizing reactance

R_s = stator resistance

R_r = rotor resistance

V_{qs} = q – axis stator voltage

V_{ds} = d – axis stator voltage

V'_{qr} = q – axis rotor voltage

V'_{dr} = d – axis rotor voltage

P = number of poles

p (small case) = differential operator ($\frac{d}{dt}$)

J = moment of inertia (kg-m²)

T_e = electromagnetic torque

T_L = load torque

ω_b = motor base electrical speed

ω_r = rotor electrical speed

$L_r = L_{lr} + L_m$;

$T_r = L_r / R_r$;

$w_b = 2 * \pi * f_b$

$X_{ls} = w_b * L_{ls}$

$X_{lr} = w_b * L_{lr}$

$X_m = w_b * L_m$

$X_{mstar} = 1 / ((1/X_{ls}) + (1/X_m) + (1/X_{lr}))$

MACHINE PARAMETER SPECIFICATION:

$R_r = 0.39 \Omega$;

$R_s = 0.19 \Omega$;

$L_{ls} = 0.21 \text{e-}3 \text{H}$;

$L_{lr} = 0.6 \text{e-}3 \text{H}$;

$L_m = 4 \text{e-}3 \text{H}$;

$f_b = 100 \text{Hz}$;

$p = 4$;

$J = 0.0226 \text{ kg-m}^2$;